

orientations are not related by hexagonal (or trigonal) symmetry operations and therefore the crystals are not hexagonal urea inclusion compounds. Sebaccic acid-urea crystals, on the other hand, are hexagonal and the e.s.r. spectra indicate that the sebaccic acid radical is undergoing large amplitude oscillations.<sup>19</sup> This motion removes the  $\alpha$ -proton anisotropy in a plane perpendicular to the hexagonal needle axis, and produces an easily recognizable isotropic spectrum in this plane. Similar results are obtained for 1,12-dodecanedioic acid, and crystals of sebaccic acid-urea and 1,12-dodecanedioic acid-urea are apparently urea inclusion compounds. Therefore, there is a transition from hexagonal urea inclusion crystals to crystals of lower symmetry as the saturated dicarboxylic acid chain length is shortened.<sup>26</sup> From the e.s.r. data it is evident that

(26) This transition was first noted in the series of acids: succinic acid, adipic acid, and sebaccic acid by Schlenk<sup>11</sup> from X-ray powder diffraction

some of the short-chain length acid molecules have similar orientations in the nonhexagonal crystals. In particular it is interesting to note that the orientations of the acid radicals are the same in the two crystals, succinic acid-urea and fumaric acid-urea. The positions of the urea molecules cannot be determined from e.s.r. data since urea does not produce stable paramagnetic damage sites at room temperature.

**Acknowledgments.**—We wish to thank Professor J. Holmes Sturdivant for his advice and help concerning this work, especially in relation to the Laue X-ray photography. We are also greatly indebted to Professor Harden M. McConnell for the generous use of his laboratory facilities.

data. Of course, neither the powder diffraction data nor the single crystal e.s.r. data are a substitute for a (single crystal) X-ray crystallographic investigation. However, e.s.r. does provide a method for investigating the structure, positions, and molecular motion of the X-ray produced free radicals in the crystals.

[CONTRIBUTION FROM THE RADIATION LABORATORY, CONTINENTAL OIL COMPANY, PONCA CITY, OKLAHOMA]

## Mercury-Photosensitized Decomposition and Collision Broadening of Resonance Line

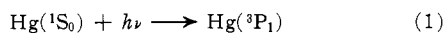
BY KANG YANG

RECEIVED MARCH 25, 1964

A low-pressure mercury lamp commonly employed in photochemical investigations emits 2537 resonance radiation with a Doppler half-breadth 4.35 times that of the absorption line. This mismatch in the two line shapes drastically reduces light absorption in spite of the high absorption coefficient; thus, a 4.8-cm. long cell with mercury at 25° absorbs only 56% of the incident light. The addition of foreign gases sharply increases the light absorption, because the absorption line becomes collision broadened. From the dependence of the light absorption on foreign gas pressures, the Lorentz half-breadths for various gases are determined under experimental conditions commonly used in photosensitized decompositions. Experimental broadening cross sections estimated from the Lorentz half-breadths agree well with theoretical ones if it is assumed that the line broadening occurs by the formation of a loosely bound activated complex. The quantum yield of hydrogen in the photosensitized decompositions of ethane, propane, *n*-butane, isobutane, and neopentane increases with increasing pressure;  $\phi^{-1} = \phi_{\infty}^{-1} + bp^{-1}$  even after making appropriate corrections for the line broadening. The high pressure limit of quantum yield,  $\phi_{\infty}$ , is found to be approximately unity for all paraffins. In the decomposition of ethylene, the correction due to the line broadening does not alter the already known rate equation,  $\phi^{-1/2} = \phi_0^{-1/2} + b'p$ . This correction, however, significantly increases the estimated lifetime of excited ethylene. The only important primary process in ethylene decomposition is the formation of molecular hydrogen, because the low pressure limit of the quantum yield,  $\phi_0$ , is found to be unity.

### Introduction

The absorption of 2537 Å. light by ground-state mercury atoms results in the following transition



Resulting excited atoms have been extensively employed to photosensitize various gas phase reactions.<sup>1</sup> Elucidation of the mechanism of these reactions often demands detailed information on the dependence of the absorption coefficient,  $k(\nu)$ , on various experimental parameters. Among them, the pressure of foreign gases is of prime importance. Most gases employed in the photosensitized reactions do not absorb at 2537 Å.; nevertheless, they profoundly affect  $k(\nu)$ , because  $k(\nu)$  becomes pressure broadened.<sup>2</sup>

Though its importance has been repeatedly emphasized,<sup>1,2</sup> the variation of  $k(\nu)$  with foreign gas pressures is usually neglected in mechanism discussions. An ap-

parent justification seems to be that, due to high  $k(\nu)$ , the light is completely absorbed; and any variation in the total amount of light absorbed is governed by the resonance lamp itself and not by possible changes in  $k(\nu)$ . This is true, provided one considers only a single frequency,  $\nu_0$ , at which  $k(\nu)$  is maximum. For example, the fraction of light passing unabsorbed through a 4.8-cm. long cell with mercury reservoir at 25° can be estimated to be only  $\exp(-38.6)$ .

More properly, however, the whole frequency range contributing to the resonance transition should be considered. Let  $E(\nu)$  be the frequency distribution of the emission line; then the transmitted light between  $\nu$  and  $\nu + d\nu$  at a path length of  $l$  cm. is  $E(\nu) \exp(-k(\nu)l)$ ; hence the absorption,  $A$ , becomes

$$A = 1 - \frac{\text{transmitted light}}{\text{incident light}} = 1 - \frac{\int_0^{\infty} E(\nu) \exp(-k(\nu)l) d\nu}{\int_0^{\infty} E(\nu) d\nu} \quad (2)$$

(1) For example, see (a) W. A. Noyes, Jr., and P. A. Leighton, "The Photochemistry of Gases," Reinhold Publishing Corp., New York, N. Y., 1941; (b) E. W. R. Steacie, "Atomic and Free Radical Reactions," Reinhold Publishing Corp., New York, N. Y., 1954.

(2) For example, see A. C. G. Mitchell and M. W. Zemansky, "Resonance Radiation and Excited Atoms," The Cambridge University Press, Cambridge, 1961.

Thus,  $A$  critically depends on how well the emission line matches the absorption line (a plot of  $k(\nu)$  vs.  $\nu$ ). Usually the emission line is much broader than the absorption line, and  $A$  is significantly less than unity. A preliminary experimental investigation indicated that  $A \approx 0.56$  instead of  $1 - \exp(-38.6)$  in the above example. The error in  $A$  arising from the neglect of the line broadening could thus amount to 79% in this case.

When the temperature of the mercury reservoir is 25° or less and foreign gas pressure does not exceed a few atmospheres, the most important process affecting  $k(\nu)$  is the Lorentz collision broadening.<sup>2,3</sup> The absorption line in this case is expressible in terms of Lorentz half-breadth  $\Delta\nu_L$ , which increases with increasing foreign gas pressure. The present paper reports these  $\Delta\nu_L$  values for various foreign gases determined under conditions commonly encountered in photosensitized decompositions.

Still another object of the present paper is to reinvestigate the photosensitized decomposition of gaseous paraffins and ethylene with appropriate corrections for the line broadening. The results for the pressure dependence of hydrogen yield indicate that this correction does not alter qualitative conclusions about the mechanism, but the estimated rate constants change significantly.

### Experimental

**A. Material.**—All hydrocarbons were Phillips research grade. The ethane contained 10<sup>-3</sup>% ethylene as the major impurity. This was removed as follows. A H<sub>2</sub>SO<sub>4</sub>-P<sub>2</sub>O<sub>5</sub> mixture was degassed by sweeping with Linde helium. The helium employed here as well as in other degassings was freed from possible impurities, such as oxygen, by passing through a spiral molecular sieve column maintained at liquid nitrogen temperature. Prior to use, all sieve columns were pumped for 12 hr. at 400°. The ethane was bubbled through the degassed H<sub>2</sub>SO<sub>4</sub>-P<sub>2</sub>O<sub>5</sub> mixture very slowly. A KOH trap and a molecular sieve trap, both at room temperature, then followed. The resulting ethane was swept through with helium for 45 min., during which the ethane was kept in liquid phase by occasional dipping in liquid nitrogen. Thorough degassing by repeated evacuation followed. No attempt was made to determine olefin content of the other paraffins; but to make sure, all the paraffins were subjected to the same treatment as the ethane. The ethylene was degassed by repeated evacuation and subjected to one stage trap-to-trap distillation, retaining the middle third. Matheson's assayed reagent rare gases and hydrogen were used without purification.

**B. Determination of the Absorption.**—An absorption cell was made by fusing two optically flat quartz windows of 5-cm. diameters at both ends of a 4.8-cm. long Vycor cylinder. The outlet to the mercury reservoir had a large diameter of 2 cm., which ensured a rapid equilibration of mercury vapor. The light source was a Hanovia low-pressure mercury lamp (94A-1) made of Vycor, which does not transmit at 1849 Å. This linear lamp had an over-all length of about 47 cm., but only the middle 5 cm. were employed in the experiments. The operating condition was very mild (575 v. and 0.120 amp.). Though no precaution was taken to cool it, the effective emitting zone had a wall temperature of 32°. The intensity of the light passing through the cell was first reduced 130 times by inserting two layers of nickel screen. The reduced light then passed a round opening of 1-cm. diameter and was projected on the phototube inlet of a Beckman DU spectrophotometer. Precautions were taken to avoid measuring scattered light.<sup>4</sup>

The resonance lamp also emits light not involved in the resonance transition. To estimate necessary corrections, a few experiments were carried out in which the same cell was placed in the spectrophotometer sample compartment while the same lamp occupied the light source. The wave length selector was positioned at 2537 Å., and the absorption experiments were repeated.

(3) For a recent review, see S. Chen and M. Takeo, *Rev. Mod. Phys.*, **29**, 20 (1957).

(4) M. W. Zemansky, *Phys. Rev.*, **36**, 919 (1930).

Transmission,  $T'$ , measured with all wave lengths is

$$T' = \frac{U_i + \Delta}{U_0 + \Delta}$$

where  $U_0$  and  $U_i$  denote the resonance light at a cell length of 0 and  $l$  (4.8 cm.) and  $\Delta$  indicates the light not involved in the transition; hence,  $A$  as defined in (2) is

$$A = 1 - \frac{U_i}{U_0} = \left(1 + \frac{\Delta}{U_0}\right) (1 - T')$$

The  $A$  determined with 2537 Å. in the presence of 600 mm. propane was 0.978. Corresponding  $T'$  was 0.175, hence  $(1 + \Delta/U_0) = 1.185$ . This factor was used throughout the experiments. Table I summarizes a typical result on the determination of  $A$ .

TABLE I  
ABSORPTION AT DIFFERENT ETHYLENE PRESSURES  
 $A = 1 - (\text{transmitted light/incident light})$

Pressure, mm.	$A$
0	0.556
10	0.752
20	0.806
30	0.856
50	0.914
70	0.939
100	0.957
150	0.968
200	0.971
300	0.974
400	0.979
600	0.980

**C. Photosensitized Decomposition.**—The photosensitized decomposition of ethylene was carried out simultaneously with the determination of  $A$ . This procedure was not convenient in paraffin decompositions where it was necessary to carry out the photosensitized decompositions at low intensity and low conversion. Here, a larger Vycor cell (140-cc. cyclinder, 5-cm. diameter) was employed with the reasonable assumption that the dependence of  $A$  on paraffin pressures was the same in both cells.

Hydrogen, the only product analyzed, was determined gas chromatographically with a homemade unit. Some precautions were needed to improve sensitivity and reproducibility. A thermistor in the sensing side of the detector was covered with a layer of nickel screen to reduce background noise. Two separate argon tanks were provided, one for the sensing side and the other for the reference side. This precaution together with the use of a large surge tank reduced pressure disturbances arising from sample injections. The signal from the thermistor was fed to a recorder through a d.c. stabilized amplifier. All power lines were controlled. Other details have been described before.<sup>5</sup> Photon input rate was determined by assuming that the high-pressure limit of hydrogen quantum yield in propane decomposition was unity. All experiments were carried out at  $25 \pm 1^\circ$ .

### Results and Discussion

**A. Lorentz Collision Broadening.**—To discuss the pressure dependence of  $A$  in terms of line broadening, it is necessary to know the explicit expressions for emission and absorption line shapes. The former is taken to be a Doppler line

$$E(\nu) = Ce^{-(\omega/\alpha)^2} \quad (3)$$

where  $C$  is a constant and

$$\omega = \frac{2(\nu - \nu_0)}{\Delta\nu_D} \sqrt{\ln 2} \quad (4)$$

$$\alpha = \Delta\nu_E/\Delta\nu_D$$

Here,  $\Delta\nu_D$  is the Doppler half-breadth of the absorption line and  $\Delta\nu_E$  denotes the half-breadth of the emission

(5) K. Yang and P. L. Gant, *J. Phys. Chem.*, **65**, 1861 (1961).

line. The absorption line shape is usually derived by supposing that Lorentz collision broadening superimposes on natural damping and Doppler broadening.<sup>2,6</sup> The absorption coefficient then takes the following form

$$k(\nu) = k(\nu_0) \frac{a}{\pi} \int_{-\infty}^{\infty} \frac{e^{-y^2} dy}{a^2 + (\omega - y)^2} \quad (5)$$

where  $k(\nu_0)$  is the absorption coefficient at the maximum absorption and

$$a = \frac{\Delta\nu_N + \Delta\nu_L}{\Delta\nu_D} \sqrt{\ln 2} \quad (6)$$

Here,  $\Delta\nu_N$  denotes natural damping half-breadth. Within the present pressure range,  $\Delta\nu_L \gg \Delta\nu_N$ ; hence the latter is neglected when the collision broadening occurs. From (2), (3), and (5)

$$A = 1 -$$

$$\left[ \int_{-\infty}^{\infty} \exp(-\omega^2/\alpha^2) \exp \left\{ -k(\nu_0)l \frac{a}{\pi} \int_{-\infty}^{\infty} \exp(-y^2) \times (a^2 + (\omega - y)^2)^{-1} dy \right\} d\omega / \int_{-\infty}^{\infty} \exp(-\omega^2/\alpha^2) d\omega \right] \quad (7)$$

As shown in Appendix I,  $\alpha$  is determined by Zemansky's method<sup>4</sup> and found to be 4.35. In the present experiment,  $k(\nu_0)l = 38.6$ . With these data, (7) is numerically integrated by using an IBM 7090 computer. The resulting  $A$  values at various  $a$  are summarized in Table II. Using these data,  $a$  (hence  $\Delta\nu_L$

TABLE II  
ABSORPTION AT DIFFERENT LORENTZ HALF-BREADTHS  
 $a = \Delta\nu_L \sqrt{\ln 2} / \Delta\nu_D$ ;  $k(\nu_0)l = 38.6$ ;  $\alpha = 4.35$   
 $A = 1 - (\text{transmitted light/incident light})$

$a$	$A$	$a$	$A$
0.00	0.4868	0.50	0.8055
0.05	0.5821	1.00	0.8864
0.10	0.6216	1.50	0.9219
0.15	0.6578	2.00	0.9403
0.20	0.6891	2.50	0.9504
0.25	0.7159	3.00	0.9558
0.30	0.7390	3.50	0.9580
0.35	0.7590	4.00	0.9578
0.40	0.7764	4.50	0.9556
0.45	0.7918	5.00	0.9518

also) can be estimated from experimentally determined  $A$ .<sup>4</sup> This procedure is found to be unreliable when a foreign gas pressure exceeds about 100 mm. where small  $A$  accompanies too much  $\Delta a$ .

In Fig. 1, some  $a$  values are plotted against foreign gas pressures. The linear increase is consistent with the Lorentz theory,<sup>2</sup> which demands that

$$\begin{aligned} \Delta\nu_L &= \frac{1}{\pi} [\text{no. of collisions/sec./atom}] \quad (8) \\ &= \frac{1}{\pi} \sigma_L^2 n [8\pi RT/\mu]^{1/2} \end{aligned}$$

where  $\sigma_L^2$  is the broadening cross section,  $\mu$  signifies reduced mass, and  $n$  is the number of foreign gas molecules per cc. The lines, however, do not pass through

(6) V. Weisskopf, *Z. Physik*, **75**, 287 (1932).

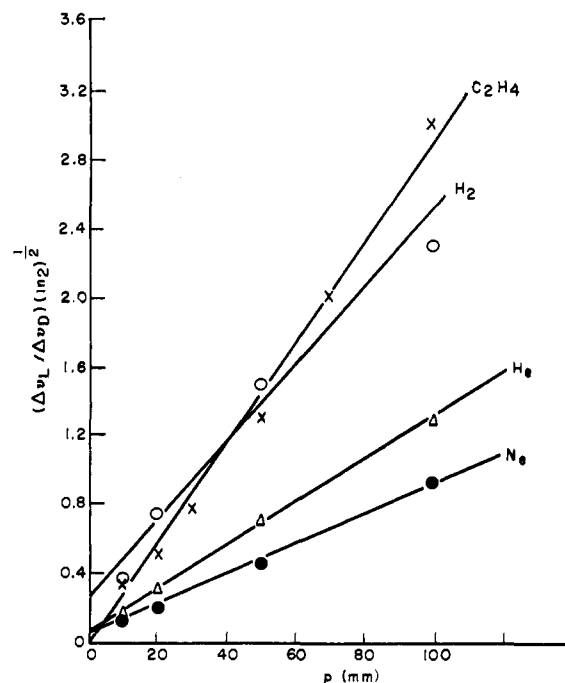


Fig. 1.—Dependence of Lorentz half-breadth on foreign gas pressures.

the origin which has been attributed to the neglect of line asymmetry.<sup>4</sup>

Table III summarizes  $\sigma_L^2$  for various foreign gases de-

TABLE III  
COLLISION BROADENING CROSS SECTIONS FOR VARIOUS FOREIGN GASES

Compd.	$\sigma^2$ , Å. <sup>2</sup>
He	37
Ne	54
A	108
Kr	135
H <sub>2</sub>	37
C <sub>2</sub> H <sub>6</sub>	127
C <sub>3</sub> H <sub>8</sub>	194
<i>n</i> -C <sub>4</sub> H <sub>10</sub>	209
<i>i</i> -C <sub>4</sub> H <sub>10</sub>	142
C <sub>2</sub> H <sub>4</sub>	223

termined from the slope of straight lines, such as shown in Fig. 1. Using an ideal resonance lamp emitting a sharp line with  $\Delta\nu_E/\Delta\nu_D = 1.21$ , Zemansky<sup>4</sup> reported that  $\sigma_L^2(\text{H}_2) = 24.5 \text{ \AA.}^2$ , while the use of a cooled discharge tube gave  $\sigma_L^2(\text{H}_2) = 53.1 \text{ \AA.}^2$  for Hg<sup>202</sup> species.<sup>7,8</sup> The present result of  $37 \text{ \AA.}^2$  is within this range.

According to the absolute rate theory,<sup>9</sup> reactions involving no activation energy proceed by the formation of a loosely bound activated complex in which internal degrees of freedom of original reactants hardly change. It is reasonable to suppose such a complex in the broadening process. When the potential energy between an excited mercury atom and a foreign gas molecule is taken as

$$V(r) = -C/r^S \quad S > 2 \quad (9)$$

(7) K. R. Osborne, C. C. McDonald, and H. E. Gunning, *J. Chem. Phys.*, **26**, 124 (1957).

(8) A good review is available on the role of line broadening in the photochemical separation of mercury isotopes: H. E. Gunning and O. P. Strausz, "Advances in Photochemistry," W. A. Noyes, Jr., G. S. Hammond, and J. N. Pitts, Jr., Eds., Interscience Publishers, Inc., New York, N. Y., 1963.

(9) S. Glasstone, K. Laidler, and H. Eyring, "The Theory of Rate Processes," McGraw-Hill Book Co., Inc., New York, N. Y., 1941, pp. 220-222.

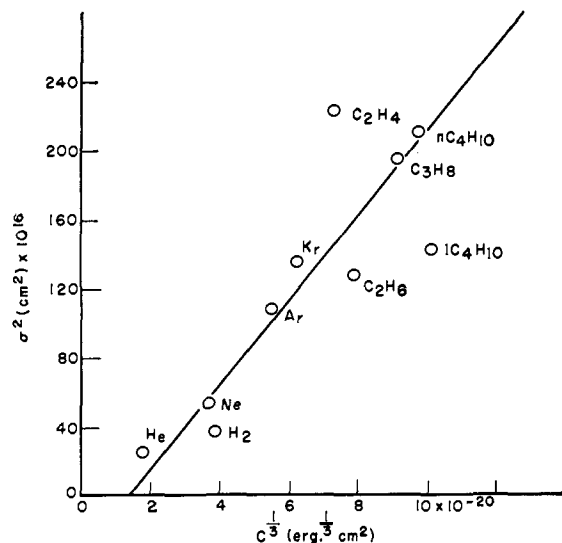


Fig. 2.—Effect of intermolecular potential ( $-C/r^6$ ) on the collision broadening cross section.

then the rate constant for the collisional interruption of light emission becomes<sup>10</sup>

$$k' = (\beta/\sqrt{\mu})(kT)^{(S-4)/2S} C^{2/S} \quad (10)$$

where  $\beta$  is a dimensionless constant defined as

$$\beta = \pi^{1/2} 2^{(3S-4)/2S} S(S-2)^{(2-S)/S} \Gamma(2-2/S) \quad (11)$$

Equating (11) with kinetic theory rate constant, it can readily be seen that

$$\sigma_L^2 = \beta(8\pi)^{-1/2} (kT)^{-1/2} C^{1/2} \quad (12)$$

Thus,  $\sigma_L^2$  should increase with the  $1/2$  power of  $C$ . The values of  $C$  can be estimated from the relations<sup>11</sup>

$$C(\text{Hg-M}) = [C(\text{Hg-Hg})C(\text{M-M})]^{1/2} \quad (13)$$

$$C(\text{M-M}) = 4\epsilon\sigma^6 \quad (14)$$

where  $\epsilon$  and  $\sigma$  are the force constant of Lennard-Jones potential and  $M$  denotes a foreign gas;  $\epsilon$  and  $\sigma$  estimated from viscosity data are used, while  $C(\text{Hg-Hg})$  is taken to be  $255 \times 10^{-60}$  erg-cm.<sup>6</sup>

In Fig. 2,  $\sigma_L^2$  is plotted against  $C^{1/2}$ . Apparently, the line does not pass through the origin, which is not explainable by the present theory. The slope of the line to which more significance should be attached is found to be  $(2.1 \pm 0.5) \times 10^5$ . The theoretical value estimated from (12) with van der Waal's dispersion force is  $3.1 \times 10^5$ . The agreement is quite good.

In principle, information on  $\Delta\nu_L$  suffices to calculate  $A$  at different foreign gas pressures. Figure 3 shows such an attempt with ethane as a foreign gas. Calculated  $A$  is lower throughout. This discrepancy in the region of pressures lower than 200 mm. comes from taking  $\sigma_L^2 = (\text{constant}) \times p$  instead of  $\sigma_L^2 = \text{constant} \times p + \text{constant}$ , as indicated in Fig. 1. When this is properly considered, agreement is quite good up to 200 mm.; but the discrepancy at higher pressures still exists. This is attributable to the neglect of line asymmetry. Collision broadening is always accompanied with a line shift,  $\Delta\nu_S$ , whose absolute value increases

(10) K. Yang and T. Ree, *J. Chem. Phys.*, **35**, 588 (1961).

(11) J. O. Hirschfelder, C. F. Curtiss, and R. B. Bird, "Molecular Theory of Gases and Liquids," John Wiley and Sons, Inc., New York, N. Y., 1954, pp. 963-966, 1110-1112.

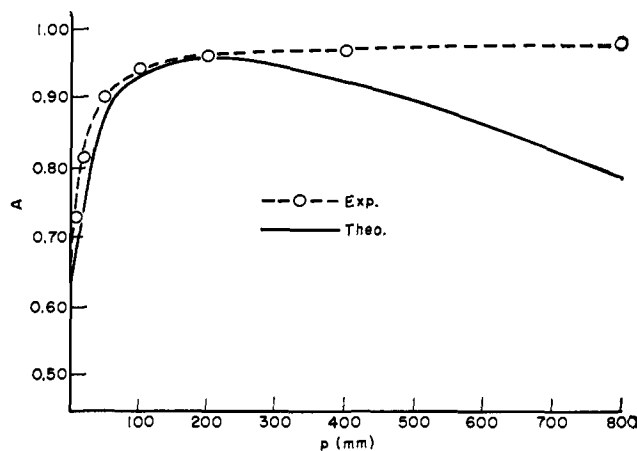


Fig. 3.—Absorption at different ethane pressures.

with increasing  $\Delta\nu_L$  (hence with pressure)<sup>2</sup>

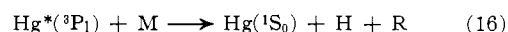
$$\frac{\Delta\nu_S}{\Delta\nu_L} = -\frac{1}{2} \tan \frac{\pi}{S-1} \quad (15)$$

where  $S$  is a potential parameter in (9). A similar asymmetry is likely to be present in  $E(\nu)$ , and additional light absorption should occur as  $\Delta\nu_S$  in  $k(\nu)$  approaches that in  $E(\nu)$ .

Equation 7 is useful in estimating an intensity distribution within a cell. This information is indispensable in treating some photolysis mechanisms, such as the diffusion of H atoms to a cell wall. Such a calculation is performed on the system with 100 mm. ethane. The result indicates that only 0.65 cm. is needed to reduce the intensity one-half. This drastic variation must always be considered in discussing intensity-dependent reactions.<sup>12</sup>

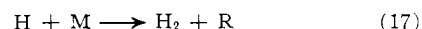
#### B. Photosensitized Decomposition of Paraffins.—

The only important primary process in the mercury photosensitized decomposition of paraffins is C-H bond rupture<sup>13</sup>

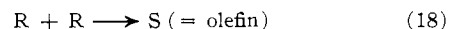


The quantum yield of H atoms in the decomposition of methane increases with increasing pressure.<sup>14</sup> A slight increase is also reported in the decomposition of *n*-butane.<sup>15</sup> Undoubtedly, the line broadening contributes to this increase. We demonstrate below, however, that there exists an increase in paraffin decompositions even after making appropriate corrections for the line broadening.

The quantum yield of hydrogen atoms,  $\phi(\text{H})$ , is usually determined by measuring the quantum yield of hydrogen molecules



In doing so, extra care must be taken to avoid internal scavenging<sup>13a,14,16</sup>



(12) G. J. Mains and H. Niki, a paper presented at the 145th National Meeting of the American Chemical Society, New York, N. Y., September, 1963.

(13) For example, see: (a) R. A. Back, *Can. J. Chem.*, **37**, 1834 (1959); (b) R. A. Holroyd and G. W. Klein, *J. Phys. Chem.*, **67**, 2273 (1963).

(14) R. A. Back and D. van der Auwera, *Can. J. Chem.*, **40**, 2339 (1962).

(15) K. R. Jennings and R. J. Cvetanović, *J. Chem. Phys.*, **36**, 1233 (1961).

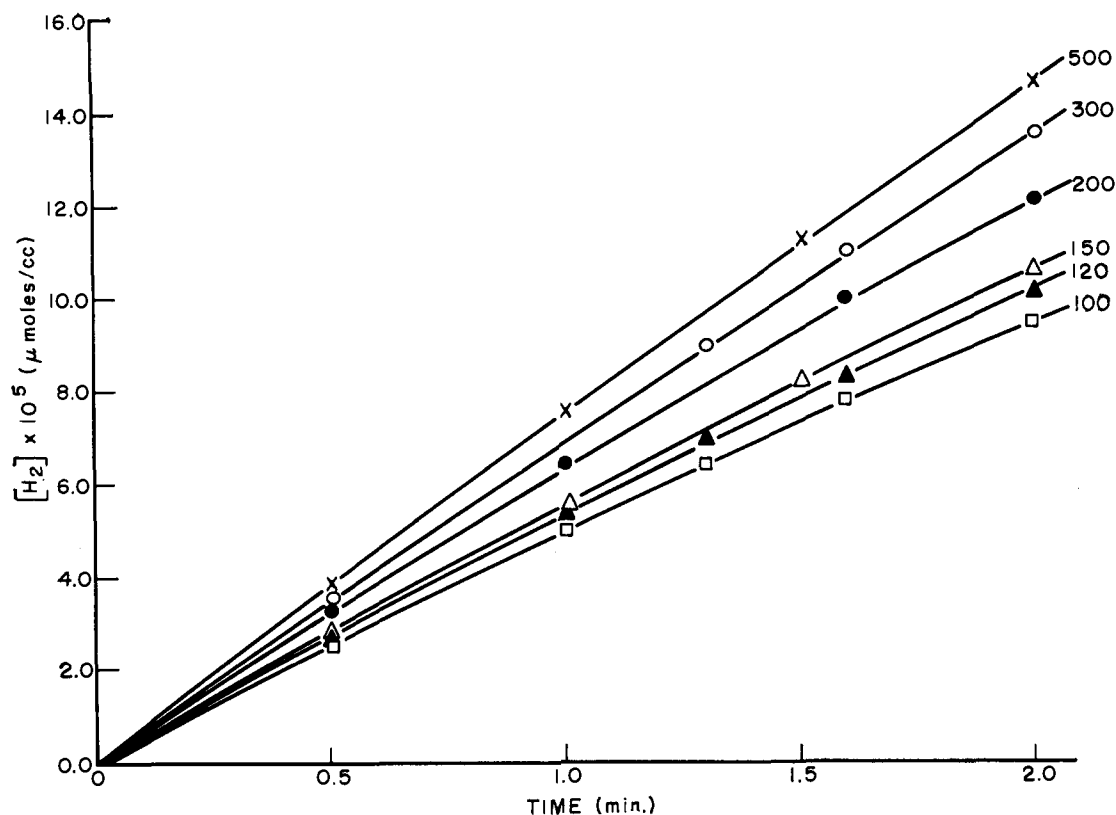


Fig. 4.—The rate curves in ethane decomposition; the numbers in each curve indicate ethane pressures in mm.

When internal scavenging occurs,  $\phi(\text{H}_2)$  decreases with increasing conversion. In the decompositions of propane, *n*-butane, and isobutane, no difficulty is encountered in determining initial  $\phi(\text{H}_2)$ . In the decomposition of ethane and neopentane, however, the quantum yields are significantly affected by conversions as low as  $1 \times 10^{-3}\%$ , as shown for ethane in Fig. 4. The rate equation which is derived in Appendix II is well suited for the determination of initial  $\phi(\text{H}_2)$  from low conversion data such as in Fig. 4

$$t = \xi x - \eta(1 - e^{-\zeta x}) \quad (21)$$

where  $t$  is irradiation time,  $x = [\text{H}_2]/[\text{M}]$ , and  $\xi$ ,  $\eta$ , and  $\zeta$  are constants. When  $x$  is small, (21) may be expanded to give

$$t = \frac{1}{r_{16}} [\text{H}_2] + \xi' [\text{H}_2]^2 \quad (22)$$

where  $\xi' = (1/r_{16}[\text{M}])(k_{20}/k_{17})f$ ,  $r_i$  and  $k_i$  denote the rate and the rate constant of reaction  $i$ , and  $f$  represents the fraction of alkyl radical ending up as olefin. The two constants,  $r_{16}$  and  $\xi'$ , are estimated by least-squares treatment. In doing so, the third-order term in (22) is always retained; and those data showing significant contribution from this term are all discarded. This practice limited the rate study to the range of ethane pressure larger than 100 mm. Figure 4 shows how well calculated solid curves fit the experimental data.

Table IV summarizes the rate data in the decomposition of ethane. With increasing pressure,  $r_{16}$  undoubtedly increases. From  $\xi'$ ,  $f(k_{20}/k_{17})$  may be estimated. Large scattering in the fourth column comes from the fact that  $f(k_{20}/k_{17})$  is estimated from very small corrections in the rate curves; nevertheless, the magnitude

Pressure, mm.	$r_{16}^a \times 10^8$	$\xi'^a \times 10^{-6}$	$f(k_{20}/k_{17}) \times 10^{-2}$	$\phi(\text{H}_2)$ , uncor.	$\phi(\text{H}_2)$ , cor.
100	5.32	23.6	7	0.554	0.581
128	5.77	22.8	9	0.601	0.630
150	5.93	17.8	8	0.618	0.638
200	6.87	16.8	12	0.716	0.732
300	7.13	5.13	6	0.743	0.752
500	7.90	7.32	16	0.823	0.827

<sup>a</sup> Concentration in  $\mu\text{moles/cc.}$  and time in min.

is reasonable. Ethane radiolysis data<sup>5</sup> indicate that  $f = 0.4$ , while photolysis data give  $f = 0.1$ .<sup>13a</sup> Taking  $f$  to be 0.3, use of an average value ( $= 10$ ) for  $f(k_{20}/k_{17})$  gives  $k_{20}/k_{17} = 3 \times 10^4$ . Reported literature values<sup>5,13a,16</sup> range  $(2.5-4.0) \times 10^4$ . As shown in fifth and sixth columns in Table IV, the correction due to the line broadening significantly alters  $\phi(\text{H}_2)$ . A few experiments have also been carried out at an intensity of  $9.00 \times 10^{-7}$   $\mu\text{mole of photons/cc./min.}$ , which is about 100 times less than that employed to obtain the data in Table V. At this intensity,  $r_{16}$  at the ethane pressure

TABLE V  
PRESSURE DEPENDENCE OF THE HYDROGEN QUANTUM YIELDS IN PARAFFIN PHOTOLYSIS

Compd.	$\phi_\infty$	$b$ , mm.
C <sub>2</sub> H <sub>6</sub>	$0.92 \pm 0.04$	$64 \pm 6$
C <sub>3</sub> H <sub>8</sub>	$1.00 \pm 0.00$	$12.4 \pm 0.4$
<i>n</i> -C <sub>4</sub> H <sub>10</sub>	$1.00 \pm 0.01$	$2.9 \pm 0.3$
<i>i</i> -C <sub>4</sub> H <sub>10</sub>	$1.00 \pm 0.01$	$2.1 \pm 0.4$
neo-C <sub>5</sub> H <sub>12</sub>	$0.86 \pm 0.02$	$87 \pm 3$
neo-C <sub>5</sub> H <sub>12</sub> , uncor.	$0.87 \pm 0.02$	$98 \pm 4$

of 100 mm. was  $5.24 \times 10^{-13}$  mole/cc./min.; thus the ratio,  $\phi$  (low intensity)/ $\phi$  (high intensity), is 1.05,

(16) K. Yang, *J. Phys. Chem.*, **67**, 562 (1963).

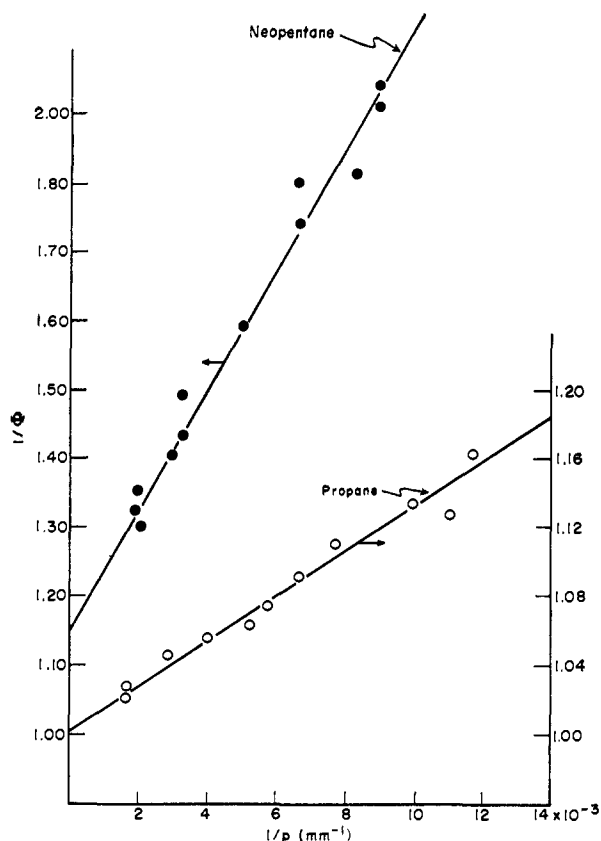


Fig. 5.—Pressure dependence of the quantum yield of hydrogen in the decomposition of neopentane and propane.

which indicates that  $\phi(\text{H}_2)$  is essentially intensity independent.

The nature of the olefin formed in neopentane decomposition is uncertain. In addition, the reaction



may occur, thus complicating the rate equation.<sup>15</sup> Because of these uncertainties, no attempt is made to use the rate equation. Instead,  $\tau_{16}$  is determined from the visual extrapolation of rate curves to zero time; hence the neopentane data to be reported below are most inaccurate.

In all paraffin decompositions, reciprocal quantum yield is found to increase linearly with reciprocal pressure

$$\phi^{-1} = \phi_{\infty}^{-1} + b p^{-1} \quad (23)$$

where  $\phi_{\infty}$  denotes the high pressure limit of quantum yield and  $b$  represents an empirical constant. Two such examples are shown in Fig. 5. Table V summarizes  $\phi_{\infty}$  and  $b$  estimated by least-squares treatment. Error ranges here are standard deviations. Since  $\phi_{\infty}$  is close to unity, the standard deviation in  $\phi_{\infty}$  is about the same as that in  $\phi_{\infty}^{-1}$ . Somewhat lower  $\phi_{\infty}$  ( $= 0.86$ ) in neopentane decomposition<sup>17</sup> may partially be due to inaccuracy in initial rates; otherwise the present data strongly indicate that C-H bond rupture occurs with quantum yield close to unity. A previous report<sup>18</sup> on the very low yield  $\phi(\text{H}_2)$  ( $= 0.0045$ ) in neopentane decomposition is not confirmed. Internal scavenging and radical recombination could have played the major

(17) Dr. H. E. Gunning (University of Alberta) kindly informed us that the  $\phi_{\infty}$  value of 0.86 is in good agreement with the result recently obtained in his laboratory.

(18) B. de B. Darwent and E. W. R. Steacie, *Can. J. Res.*, **27B**, 181 (1949).

role in reducing  $\phi(\text{H}_2)$ . Neopentane behaves very much like ethane, and peculiarities attributed to high symmetry do not exist. Various mechanisms leading to the pressure dependence have been already considered.<sup>14</sup>

C. Photosensitized Decomposition of Ethylene.—Table VI summarizes the rate data in the decomposi-

TABLE VI  
HYDROGEN FORMATION IN ETHYLENE DECOMPOSITION

Pressure, mm.	Time, sec.	H <sub>2</sub> , moles/cc., × 10 <sup>8</sup>
10	60	4.08
10	90	6.15
10	120	8.16
(6.81 ± 0.01 × 10 <sup>-11</sup> mole/cc. sec.)		
100	60	1.19
100	90	1.75
100	120	2.41

(1.99 ± 0.02 × 10<sup>-11</sup> mole/cc. sec.)

tion of ethylene. The rate is independent of conversion but decreases with increasing pressure as reported before.<sup>19</sup> An attempt was made to determine  $\phi(\text{H}_2)$  at 13 mm. of ethylene. The rate of ethylene decomposition was 0.456 times that in propane decomposition at 600 mm. At 600 mm.,  $\phi(\text{H}_2)$  in propane decomposition was 0.980; hence  $\phi(\text{H}_2)$  in ethylene decomposition with no correction for the line broadening becomes 0.447. With the correction for the line broadening, this value increases to 0.570. This clearly indicates that the line broadening must be always considered in using secondary dosimeters. The present  $\phi(\text{H}_2)$  of 0.570 at 13 mm. is higher than  $\phi(\text{C}_2\text{H}_2)$  of 0.37 at the same pressure.<sup>19</sup> The discrepancy, however, may not be real, since no correction due to the line broadening has been made in the latter value.

Table VII summarizes  $\phi(\text{H}_2)$  at different ethylene

TABLE VII  
PRESSURE DEPENDENCE OF  $\phi(\text{H}_2)$  IN ETHYLENE DECOMPOSITION

Pressure, mm.	$\phi(\text{H}_2)$ , uncor.	$\phi(\text{H}_2)$ , cor.
10	0.584	0.594
13	0.570	0.570
20	0.527	0.502
30	0.453	0.391
50	0.337	0.283
70	0.253	0.206
100	0.171	0.137
150	0.100	0.0795
200	0.0659	0.0521
300	0.0345	0.0271
400	0.0197	0.0154
600	0.0099	0.0077

pressures. Both corrected and uncorrected  $\phi(\text{H}_2)$  are found to obey the empirical relation<sup>20</sup>

$$\phi^{-1/2} = \phi_0^{-1/2} + b' p \quad (24)$$

Least-squares treatment gives for corrected  $\phi(\text{H}_2)$

$$\phi^{-1/2} = (1.04 \pm 0.03) + (1.72 \pm 0.01) \times 10^{-2} p$$

and for uncorrected  $\phi(\text{H}_2)$

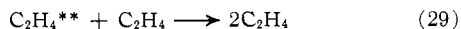
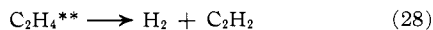
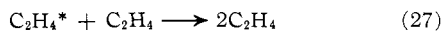
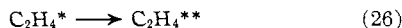
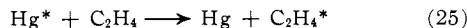
$$\phi^{-1/2} = (1.03 \pm 0.04) + (1.50 \pm 0.02) \times 10^{-2} p$$

Significantly, the low-pressure limit of  $\phi(\text{H}_2)$  is close to

(19) D. J. LeRoy and E. W. R. Steacie, *J. Chem. Phys.*, **9**, 829 (1941).

(20) A. B. Callear and R. J. Cvetanović, *ibid.*, **24**, 873 (1956).

unity in agreement with the mass spectrometric data, indicating that the only primary process in ethylene decomposition is the formation of molecular hydrogen.<sup>21</sup> Equation 24 is consistent with the following mechanism<sup>20</sup>



provided  $k_{26}/k_{27} = k_{28}/k_{29}$ . According to the above mechanism,  $b'$  in (24) is given as  $k_{29}/(k_{28}\phi_0^{1/2})$ . Taking  $k_{29} = 1 \times 10^{-10}$  (molecules/cc.)<sup>-1</sup> sec.<sup>-1</sup>, the mean life of excited ethylene estimated from corrected  $\phi(\text{H}_2)$  is  $5.1 \times 10^{-9}$  sec., while that resulting from uncorrected  $\phi(\text{H}_2)$  is 12% lower ( $4.5 \times 10^{-9}$  sec.). We thus conclude that, in the mercury photosensitized decomposition of paraffins and ethylene, the correction due to the resonance line broadening does not alter qualitative conclusions; nevertheless, it must be taken into account in quantitative discussion of the mechanism.

**Acknowledgment.**—Dr. F. H. Dickey and Dr. L. O. Morgan offered valuable discussion; Mr. J. Paden and Mr. C. L. Hassell developed the computer program for estimating  $A$ ; Dr. D. Cooper offered the computer program used in the linear and nonlinear least-squares treatment; and Mr. J. D. Reedy helped with experimental work. The author gratefully acknowledges this assistance.

### Appendix I

In the present work, the emission line is presumed to be a Doppler line

$$E(\nu) = Ce^{-(\omega/\alpha)^2}$$

$\alpha$  in this expression can be estimated by considering  $A$  in the absence of any foreign gas; then  $\Delta\nu_L = 0$ , and  $a$  given in (6) is equal to  $\Delta\nu_N\sqrt{\ln 2}/\Delta\nu_D = 0.0012$ . Using (7),  $A$  can now be calculated at different  $\alpha$ . Some numerical results are given

$\alpha$	3.0	3.5	4.0	4.5
$A$	0.7036	0.6425	0.5882	0.5440

In the present work,  $A = 0.556$  which corresponds to the  $\alpha$  value of 4.35. In the Hanovia lamp, some self-reversal is likely to be present; but (3) does not take into account this fact. The self-reversal most drastically modifies the center portion of the emission line. In most photochemical experiments,  $k(\nu_0)l$  is quite large, say above 10, and this portion is likely to be completely absorbed; hence the explicit form of  $E(\nu)$  there is probably unimportant. In this connection, it is illuminating to draw the emission and absorption lines, as shown in Fig. 6. Regardless of the nature of broadening processes which affect  $k(\nu)$ , the area under the absorption curve remains constant and is equal to  $\pi^{1/2}$ , because

$$\int_0^\infty k(\nu)d\nu = \left(\frac{\pi}{4 \ln 2}\right)^{1/2} k(\nu_0)\Delta\nu_D$$

and  $\omega$  is related to  $\nu$  by (4). In drawing the emission line,

(21) F. P. Lossing, D. G. H. Marden, and J. B. Farmer, *Can. J. Chem.*, **34**, 701 (1956).

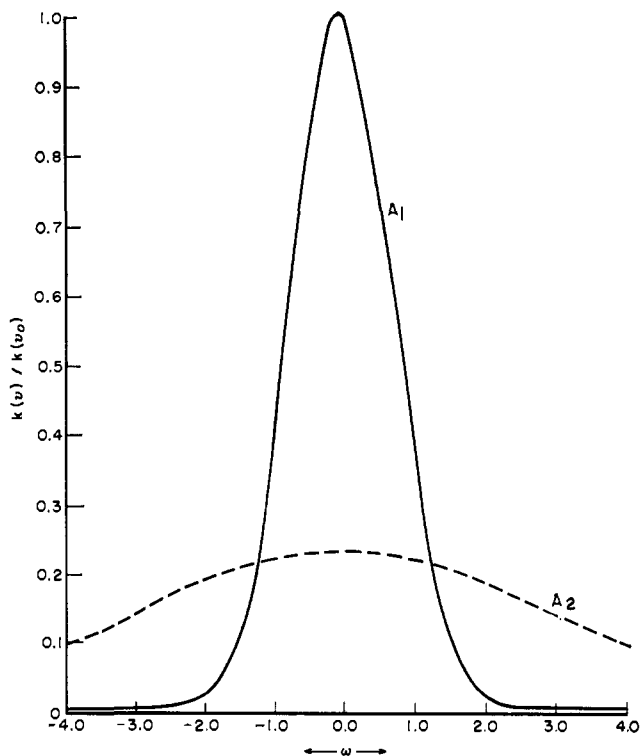


Fig. 6.—The shape of absorption and emission lines;  $A_1$  = absorption line,  $A_2$  = emission line.

$C$  in (3) is taken to be  $1/\alpha$  so that the area under both curves becomes equal. The two curves do not match well, and significant fraction of the emission line lies in the region where  $k(\nu)$  is nearly zero. It should also be noted that an explicit form of  $E(\nu)$  in the range  $-1 < \omega < +1$  is unimportant because the light there is nearly completely absorbed.

### Appendix II

Rate equation 21 is derived below. Referring to reactions 16–20, it can readily be seen that

$$\frac{d}{dt} [\text{H}_2] = \frac{r_{16}}{1 + k_{20}[\text{S}]/k_{17}[\text{M}]}$$

To express  $[\text{S}]$  as a function of  $[\text{H}_2]$  and  $t$ , we note that  $[\text{S}]$  remaining after  $t$  is equal to  $[\text{S}]_f$  formed in this period minus  $[\text{S}]_d$  consumed in the same period.

$$[\text{S}] = [\text{S}]_f - [\text{S}]_d$$

The formation of  $\text{S}$  always involves alkyl radicals. Let  $R$  be the total alkyl radicals formed in  $t$  and  $f$  be the fraction of alkyl radicals ending up as  $\text{S}$ . Similarly, we define  $R^*$  and  $f^*$  as the vibrationally excited alkyl radicals formed in (20); then material balance demands that

$$\begin{aligned} [\text{S}]_f &= fR + f^*R^* \\ &= f(r_{16}t + [\text{H}_2]) + f^*(r_{16}t - [\text{H}_2]) \end{aligned}$$

and

$$[\text{S}]_d = r_{16}t - [\text{H}_2]$$

Thus

$$\frac{d}{dt} [\text{H}_2] = \frac{r_{16}}{1 + g[\text{H}_2] - ht}$$

where  $g = (k_{20}/k_{17}[M])(1 + f - f^*)$  and  $h = (r_{16}k_{20}/k_{17}[M])(1 - f - f^*)$ . We make the reasonable approximation that  $f$  and  $f^*$  are independent of  $t$ ; then integration of the above expression gives (21), where  $\xi = ([M]r_{16})(1 + f - f^*)/(1 - f - f^*)$ ,  $\eta = (k_{17}[M]/k_{20}r_{16})(2f)/(1 - f - f^*)^2$ , and  $\zeta = (k_{20}/k_{17})(1 - f - f^*)$ . The low conversion approximation (22) does not contain  $f^*$ . This indicates that, to an approximation correct up to  $[H_2]^2$ , the hot radical effect can be neglected. Equa-

tion 22 can also be derived from the eq. 7 of a paper by Cvetanović, Falconer, and Jennings<sup>22</sup> with the approximations that  $0li = 0$  and  $k_7 = 0$ . In this connection, it should be noted that  $f = (1/2)[k_{18}/(k_{18} + k_{19})]$ . Here the numerical factor,  $1/2$ , is necessary, because only one-half of the alkyl radicals undergoing disproportionation reaction finally ends up as olefins.

(22) R. J. Cvetanović, W. E. Falconer, and K. R. Jennings, *J. Chem. Phys.*, **35**, 1225 (1961).

[CONTRIBUTION FROM THE DEPARTMENT OF CHEMISTRY, BOSTON UNIVERSITY, BOSTON, MASSACHUSETTS]

## The Radiolysis of Methanol and Methanolic Solutions. III. The Effect of Oxygen on the Radiolysis of Liquid Methanol by $^{60}\text{Co}$ $\gamma$ -Rays and by $^{10}\text{B}(n,\alpha)^7\text{Li}$ Recoils<sup>1,2</sup>

BY SANG UP CHOI AND NORMAN N. LICHTIN

RECEIVED APRIL 30, 1964

Vapor phase chromatography was used to determine yields of gaseous products. Yields of products per 100 e.v. absorbed obtained by  $\gamma$ -radiolysis *in vacuo* are:  $\text{H}_2$ , 5.0;  $\text{CH}_4$ , 0.43;  $\text{C}_2\text{H}_6$ , 0.006;  $\text{C}_2\text{H}_4$ , 0.004;  $\text{CO}$ , 0.06;  $\text{CH}_2\text{O}$ , 2.2; and  $(\text{CH}_2\text{OH})_2$ , 3.2. Yields per 100 e.v. obtained by recoil radiolysis *in vacuo* are:  $\text{H}_2$ , 5.5;  $\text{CH}_4$ , 0.66;  $\text{C}_2\text{H}_6$ , 0.04;  $\text{C}_2\text{H}_4$ , 0.04;  $\text{CO}$ , 1.0;  $\text{CH}_2\text{O}$ , 3.0; and  $(\text{CH}_2\text{OH})_2$ , 0.87. In the presence of  $\text{O}_2$ ,  $G(\text{H}_2)$ ,  $G(\text{CH}_2\text{OH})_2$ , and  $G(\text{CH}_4)$  decrease, while  $G(\text{CH}_2\text{O})$  increases. Products formed in the presence of  $\text{O}_2$ , but not in its absence, include  $\text{CO}_2$ ,  $\text{HCO}_2\text{H}$ ,  $\text{H}_2\text{O}_2$ , and probably  $\text{CH}_3\text{OOH}$ .  $G(\text{CO})$  from  $\gamma$ -radiolysis is increased by  $\text{O}_2$  but is decreased in the case of recoil radiolysis. Limiting yields of products are obtained at concentrations of  $\text{O}_2$  of the order of  $1 \times 10^{-3}$  mole  $\text{l}^{-1}$  or less. Important limiting yields per 100 e.v. from  $\gamma$ -radiolysis include:  $\text{H}_2$ , 1.9;  $\text{CH}_4$ , 0.18;  $\text{CO}$ , 0.09; peroxide, 3.1;  $\text{CH}_2\text{O}$ , 8.7;  $(\text{CH}_2\text{OH})_2$ , 0.1; and  $\text{HCO}_2\text{H}$ , *ca.* 1.5. Important limiting yields per 100 e.v. from recoil radiolysis include:  $\text{H}_2$ , 2.4;  $\text{CH}_4$ , 0.6;  $\text{CO}$ , 0.8; peroxide, 1.5;  $\text{CH}_2\text{O}$ , 3.9;  $(\text{CH}_2\text{OH})_2$ , 0.4; and  $\text{HCO}_2\text{H}$ , *ca.* 1.0. The  $\gamma$ -radiolysis data are consistent with a mechanism which assumes that only molecular products in unreactive states and free radicals diffuse into bulk solution from the spurs and which does not involve chain autoxidation of methanol. Radical and "molecular" yields relating to the proposed mechanism can be estimated. In contrast, the recoil radiolysis data cannot be explained entirely in terms of free radicals and unreactive molecular products. The data can be rationalized by assuming that metastable, excited methanol molecules also diffuse into bulk solution. The various relevant "molecular" and radical yields can also be estimated for recoil radiolysis.

### Introduction

A study of the radiolysis by X-rays and by  $^{60}\text{Co}$   $\gamma$ -rays of methanol saturated with air and with oxygen, respectively, at 1 atm. has been reported.<sup>3</sup> The extent of variation of oxygen concentration is not sufficient in this work to permit other than qualitative interpretation. In the present study, oxygen concentration was varied systematically, and both  $^{60}\text{Co}$   $\gamma$ -rays and  $^{10}\text{B}(n,\alpha)^7\text{Li}$  recoils were employed in radiolyses.

The unsatisfactory reproducibility of product yields from the  $\gamma$ -radiolysis of "pure" liquid methanol is well known.<sup>4</sup> Although this lack of reproducibility cannot be correlated with the methods of analysis employed, improvement in analytical reliability was sought in the present case through vapor phase chromatographic determination of gaseous products. In addition, further attention was directed toward achieving the complete degassing of radiolyzed methanol, in accord with the experience of Theard and Burton.<sup>5</sup>

### Experimental

**Materials.**—Methanol (Eastman Organic, Spectrograde) was purified as described previously.<sup>4,6</sup> Oxygen (Matheson) was passed through a column of Ascarite and silica gel, followed by a

trap cooled by Dry Ice, before it was introduced into the vacuum line.

Methyl borate (Matheson) employed in recoil radiolysis was rectified on a Todd column. The middle fraction of distillate was further rectified under vacuum after transfer to the vacuum line. The middle third from the second distillation was stored on the vacuum line. Aliquots were transferred by distillation.

**Preparation of Oxygenated Solutions.**—The amount of oxygen transferred to a cell (containing methanol at Dry Ice temperature) was determined manometrically by difference, with the aid of a calibrated volume. The concentration of oxygen in solution at the temperature of irradiation (taken as 25°) was then calculated from the methanol volume and the known<sup>7,8</sup> solubility.

**Irradiation.**—Pyrex glass cells used for  $\gamma$ -irradiation were prepared, cleaned, and attached to the vacuum line, and methanol was transferred under vacuum from the storage system to irradiation cells, all as described previously.<sup>4</sup> The irradiation cells were sealed off from the line under vacuum and the amounts of methanol in the cells determined by weighing.<sup>9</sup>

$\gamma$ -Irradiations were carried out at about 20° in a Schwarz-Allen type  $^{60}\text{Co}$  source<sup>10</sup> for 9 to 35 min. Irradiation times as long as 70 min. were employed occasionally to facilitate analyses for minor gaseous products. Dose rates were determined by means of the aerated acid (0.8 *N* sulfuric acid) ferrous ammonium sulfate ( $10^{-3}$  mole/l.) dosimeter.<sup>4</sup> The dose rate to methanol was about  $1.8 \times 10^{17}$  e.v.<sup>-1</sup> ml.<sup>-1</sup> min.<sup>-1</sup>. The volume of methanol was 10–20 ml. in most cases. The ratio of the volume of vapor to that of the liquid was about 1:2.

Recoil radiolyses were carried out in the Brookhaven thermal neutron facility.<sup>4</sup> Quartz irradiation cells and procedures employed in filling the cells, and in irradiating and determining doses, were those reported previously.<sup>4</sup> Concentrations of

(1) Research carried out under the auspices of the U. S. Atomic Energy Commission under Contract AT(30-1)2383.

(2) Presented at the 146th National Meeting of the American Chemical Society, Denver, Colo., Jan., 1964.

(3) E. Hayon and J. J. Weiss, *J. Chem. Soc.*, 3970 (1961).

(4) M. Imamura, S. U. Choi, and N. N. Lichtin, *J. Am. Chem. Soc.*, **85**, 3565 (1963).

(5) L. M. Theard and M. Burton, *J. Phys. Chem.*, **67**, 59 (1963).

(6) The present preparation corresponds to methanol C of ref. 4.

(7) "International Critical Tables," Vol. III, McGraw-Hill Book Co., Inc., New York, N. Y., 1928, p. 262.

(8) C. B. Kretschmer, J. Nowakowska, and R. Wiebe, *Ind. Eng. Chem.*, **38**, 506 (1946).

(9) N. N. Lichtin, *J. Phys. Chem.*, **63**, 1449 (1959).

(10) H. A. Schwarz and A. O. Allen, *Nucleonics*, **12**, 58 (1954).